UNIVERSIDAD DE LA FRONTERA
Departamento de Ingeniería de Obras Civiles
Facultad de Ingeniería & Ciencias

RIOC
REVISTA INGENIERÍA DE OBRAS CIVILES

A Pressure-Sensitive Approach for Transient Analysis of Uniformly Distributed Demands.

Un Enfoque Sensible a la Presión para el Análisis Transitorio de Demandas Uniformemente Distribuidas.

INFORMACIÓN DEL ARTÍCULO

Article history:

Received
13-01-2018
Accepted
19-03-2018
Available
08-11-2018

Keywords:
Method of characteristics
Newton-Raphson
Pressure-insensitive demand
Pressure-sensitive demand
Transient flow

Historial del artículo:

Recibido
13-01-2018
Aceptado
19-03-2018
Publicado
08-11-2018

Palabras Clave:
Método de las Características
Newton-Raphson
Demanda insensible a la presión
Demanda sensible a la presión
Flujo transiente

J. Twyman[1]

[1] Twyman Ingenieros Consultores, Rancagua, Chile.
john@twyman.cl, teléfono: +56-9-89044770.

Abstract

In the modelling of water distribution systems is common to assume that water demands are located at the junctions, with a constant and previously known value. This assumption allows simplify the mathematical analysis of the problem, even though in cases of transient flow is more suitable to model the water demand assuming that it has a magnitude which is pressure-sensitive. In this article an original pressure-sensitive approach valid to calculate the transient flow condition in a pipe with uniformly distributed demands is presented. The general conclusion is that the approach based on the pressure-sensitive demand, compared with the usual method of the pressure-insensitive demand, shows significant attenuation in pressure which may condition the design and/or operating procedure of some devices such as valves or air chambers.

Resumen

En la modelación de los sistemas de distribución de agua es común suponer que las demandas de agua se ubican en los nodos donde se unen las tuberías, con un valor constante y previamente conocido. Esta hipótesis permite simplificar el análisis matemático del problema, pese a que en los casos de flujo transitorio es más adecuado modelar la demanda de agua suponiendo que tiene una magnitud sensible a la presión. En este artículo se presenta un enfoque original sensible a la presión, que es válido para calcular la condición de flujo transitorio en una tubería con demandas uniformemente distribuidas. La conclusión general es que el enfoque basado en la demanda sensible a la presión, en comparación con el método usual de la demanda insensible a la presión, muestra una atenuación significativa en la presión que puede condicionar el diseño y/o el funcionamiento de algunos dispositivos tales como válvulas o estanques hidroneumáticos.

1. Introduction.

Typically, water modeling programs assume that all demands are volume-based, and maintain the user-input demand regardless of the calculated available pressure. Although this assumption works well under the normal range of pressure conditions, it loses accuracy if an episode such as a fire or pump outage causes a significant decrease in system pressure. In this context, the assumption that all demands are fully satisfied regardless of the system pressure becomes unreasonable and represents the main limitation of the conventional demand driven analysis (DDA) approach to water distribution systems (WDS) modeling [14], being the pressure dependent analysis (PDA) superior to DDA [15], especially when conventional approach of DDA analysis cannot accurately predict the WDS behavior under pressure deficient conditions. In abnormal operating conditions, WDS may be pressure deficient and thus unable to satisfy demands in full. In such circumstances, PDA models are suitable to quantify the shortfall in flow and pressure accurately for crucial decision-making. Such scenarios cannot be simulated satisfactorily with the conventional DDA models as they do not consider the relationship between nodal flows and the available pressure [13]. There are a number of networks (irrigation, water supply networks, etc.) which do not follow some assumptions such as that water withdrawal takes place at the junctions, with fixed and known values. According to Salgado et al. [12], the first assumption is aimed at simplifying the mathematical solution of the problem, while the second has been a not always suitable standard practice since it is well known that consumption is pressure-dependent. Industrial applications, such as fire protection systems, mining heap leaching, all of them based on sprinklers that also deliver water in an amount that is pressure-dependent. In irrigation systems with sprinklers, drippers or porous devices (pots, strips), water is released in a pressure-dependent fashion; clearly in such systems the pressure-discharge relationship cannot be ignored. In water supply networks, problems such as leakage modeling and extended period simulation are also pressure-dependent. As a matter of fact most of the network operators do know that if they reduce the pressure in the distribution system the total water consumption outflow will be reduced. This leads to the standard practice of reducing night pressures in order to control system leakages. Some of available water hammer software lacks of pressure-dependent demand function to calculate the pressures within a water system, this situation could produce invalid results for certain water systems [2]. Because of the pressure-insensitive demand assumption is intrinsically inaccurate and tends to overdesign surge protection devices, in the following paragraphs a novel simple and useful algorithm for modeling the pressure-sensitive demand located in junctions using the standard MOC is presented, which allows represent the effect of pressure changes and produce more accurate transient results.

2. Material and methods

2.1 Basic equations of the transient flow

When analyzing a volume control, is possible to obtain a set of non-linear partial differential equations of hyperbolic type valid for describing the one-dimensional transient flow in pipes with circular cross-sectional area [3, 24]:

$$\frac{a^2}{gA}\frac{\partial Q}{\partial x}+\frac{\partial H}{\partial t}=0 \tag{1}$$

$$\frac{\partial Q}{\partial t}+gA\frac{\partial H}{\partial x}+\frac{f}{2DA}Q|Q|=0 \tag{2}$$

Where: (1) and (2) correspond to continuity and momentum (dynamics) equations, respectively. Besides, ∂ = partial derivative, H = hydraulic grade-line elevation, a = wave speed, g = gravity constant, A = pipe cross-sectional area, Q = fluid flow, f = friction factor (Darcy-Weisbach) and D = inner pipe diameter. The subscripts x and t denote spatial and time dimension, respectively. Equations (1) and (2), in conjunction with the equations related with the boundary conditions of specific devices, describe the phenomenon of wave propagation for a water hammer event.

2.2 Wave speed

The more general equation to calculate the wave speed in fluids without air is [16, 22-23]:

$$a^2=\frac{K/\rho}{1+[(K/E)(D/e)]c_1} \tag{3}$$

With: K = bulk modulus of the water; ρ = water density; e = pipe wall thickness; K = volumetric compressibility modulus of water; E = elasticity modulus of the pipe; c_1 = factor related with the pipe support condition, generally equal to $1-u^2$ (u = Poisson ratio of the wall material), which corresponds to pipeline anchored against longitudinal movement [23].

2.3 Method of Characteristics (MOC)

MOC is very used for solving equations that govern the transient flow because it works with a constant wave speed and, unlike other methodologies based on finite difference or finite element, it can easily model wave fronts generated by very fast transient flows. MOC works converting the computational space (x) - time

(t) grid (or rectangular mesh) in accordance with the Courant condition. It is useful for modelling the wave propagation phenomena in WDS due to its facility for introducing the hydraulic behavior of different devices and boundary conditions (valves, pumps, reservoirs, etc.). According to Karney [7] and Karney and McInnis [8], the Method of Characteristics proceeds by combining the dynamic and continuity equations together with unknown multiplier. Suitable chosen values of this multiplier allows the partial differential terms to be combined together and replaced by total differentials. When using the simplified governing equations the result of this process is:

$$\frac{dH}{dt} \pm \frac{a}{gA}\frac{dQ}{dt} + \frac{afQ|Q|}{2gDA^2} = 0 \quad (4)$$

With the associated equation ($Q/A \ll a$):

$$\frac{dx}{dt} = \pm a \quad (5)$$

The two equations associated with the positive value are usually termed the C^+ equations and the remaining two relations associated with the negative value are called the C^- equations (**Figure 1**). The head and flow values are known at time t and it is desired to know this values at time $t + \Delta t$. A typical such point is P, with unknowns H_P and Q_P.

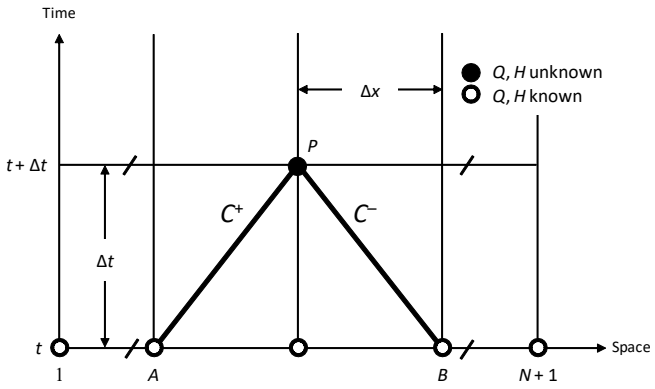

Figure 1 $x - t$ plane with Characteristics grid (adapted from [8]).

The ratio of Δx to Δt is chosen so the associated relation $dx/dt = a$ is satisfied between A and P, and $dx/dt = -a$ is satisfied between B and P. Next, equation (4) is integrated between A and P for the C^+ equation and between B and P for the C^- equation. The difficulty in this integration lies solely in the friction term, since the other terms can be evaluated exactly. The discharge in the friction term is usually simply evaluated at A or B where its value is known, which result in a first-order difference solution to equations (4) and (5). Following the notation of Wylie and Streeter [23] the procedure can be written in the following form:

$$C^+: H_P = C_P - \frac{a}{gA}Q_P \quad (6)$$

$$C^-: H_P = C_M + \frac{a}{gA}Q_P \quad (7)$$

In which:

$$C_P = H_A + \frac{a}{gA}Q_A - \frac{f\Delta x}{2gDA^2}Q_A|Q_A| \quad (8)$$

$$C_M = H_B + \frac{a}{gA}Q_B + \frac{f\Delta x}{2gDA^2}Q_B|Q_B| \quad (9)$$

For internal sections where two characteristics met, as a point P in **Figure 1**, equations (6) and (7) provide a simple solution for H_P. This can be written:

$$H_P = \frac{C_P + C_M}{2} \quad (10)$$

Q_P can then be found by back substitution into equation (6) or (7). At each end of the pipe one of equations (6) and (7) will be available. Solution for unknown head and flow at this point cannot then be obtained by the above procedure. Instead, consideration must be given to the nature of the boundary condition, which generally takes the form of a prescribed relation between head and flow. Among MOC main advantages highlighting its ease of use, speed and explicit nature, which allows calculate the variables Q and H directly from previously known values [3, 23]. The main disadvantage of MOC is to be met with the Courant stability criterion (C_n) that can limit the magnitude of the time step (Δt) common for the entire network. In order to get C_n = 1.0, some pipe initial properties can be modified (length and / or wave speed). Another way is to keep the initial conditions and apply numerical interpolations with risk of generating errors (attenuations) in the solution [4]. MOC stability criterion states that [9, 17-21]:

$$C_n = \frac{a \cdot \Delta t}{\Delta x} \leq 1.0 \quad (11)$$

Where: Δt = time step and Δx = reach length = L/N (with L = pipe length and N = number of reaches). In general, MOC gives exact numerical results when C_n = 1.0; otherwise, it generates erroneous results in form of attenuations (when $C_n < 1.0$) or numerical instability (when $C_n > 1.0$).

2.4 Simple one-node boundary condition

According to Karney [7], one the most important boundary conditions the multi-pipe frictionless junction (**Figure 2**).

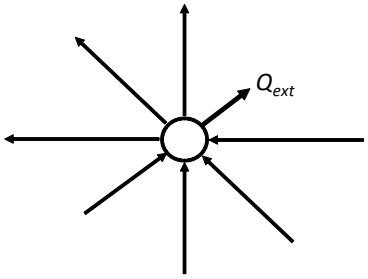

Figure 2 Ordinary node (adapted from [7, 8]).

Let N_1 be the set of all pipes whose assumed direction is toward the node in question; similarly, let N_2 be the set of all pipes whose assumed direction is away from the junction. Let one flow be identified as external and governed by an auxiliary relation. The sign convention is that positive flows are directed away from the junction being considered. The assumption that the junction is frictionless is equivalent to saying that the hydraulic grade line elevation at the node can be represented by a single number, designed H_P. For all pipes belonging to the set N_1, the C^+ characteristic equation holds, while for members of N_2 the C^- characteristic equation applies. Equations (6) and (7) can be rearranged to obtain:

$$Q_{Pi} = \frac{-H_P}{B_i} + \frac{C_{Pi}}{B_i} \qquad \forall i \in N_1 \qquad (12)$$

$$-Q_{Pj} = \frac{-H_P}{B_j} + \frac{C_{Mj}}{B_j} \qquad \forall j \in N_2 \qquad (13)$$

In which: Q_{Pi} (Q_{Pj}) represents the discharge at the boundary section of pipe i (j). The continuity equation for the junction requires the sum of the flows entering the node to equal the sum of the flows leaving the node. Thus, the continuity equation can be written:

$$\sum_i Q_{Pi} - \sum_j Q_{Pj} - Q_{ext} = 0 \qquad (14)$$

Equations (12) and (13) can be substituted directly into equation (14) and an expression for H_P is obtained. The result is:

$$H_P = C_c - B_c \cdot Q_{ext} \qquad (15)$$

Equation (15) represents the general multi-pipe junction with one external flow which allows a simple treatment of networks with complex topology [11, 25], where:

$$\frac{1}{B_c} = \sum_i \frac{gA_i}{a_i} + \sum_j \frac{gA_j}{a_j} \qquad (16)$$

$$C_c = B_c \left[\frac{gA_i}{a_i} \sum_i C_{Pi} + \frac{gA_j}{a_j} \sum_j C_{Mj} \right] \qquad (17)$$

2.5 Modelling of the pressure-sensitive demands

According to Jung et al. [6], in conventional transient models is presumed that the nodal demand is pressure-insensitive under all operating conditions, even though is known that in the actual systems the demand tends to fluctuate according to the nodal pressure. The pressure-sensitive demand can be simulated with emitters that discharge the flow to the atmosphere through a nozzle or orifice. The flow rate through the emitter varies as a function of the pressure available at the junction j and it can be expressed as [1, 6, 12]:

$$q_j = C_{\text{emit}} \cdot p_j^{\beta} \qquad (18)$$

Where q_j = flow rate (L/s) from emitter and p_j = pressure (m) at emitter. Both C_{emit} = emitter coefficient (L/s/m$^{\beta}$) and β = emitter exponent are normally provided by the emitter manufacturers or obtained via least squares fitting to field or laboratory data [12]. Using equation (18), the emitter is used to simulate the effect of the pressure-sensitive demand.

2.6 Development of the equations

Making $q_j = Q_{ext}$ and $p = (H_P - z)$ in equation (18), and replacing the resultant expression into equation (15), the following expression can be obtained:

$$H_P = C_c - B_c \cdot C_{\text{emit}} \cdot (H_P - z)_j^{\beta} \qquad (19)$$

With z = junction elevation. Re-ordering equation (19) we obtain:

$$H_P + B_c \cdot C_{\text{emit}} \cdot (H_P - z)_j^{\beta} - C_c = 0 \qquad (20)$$

The novelty that equation (20) gives is that it allows calculate the pressure-sensitive demand in any ordinary node no matter the number of pipes connected to it. Equation (20) is general because it can be reduced to equation (15) when it is assumed that demand is pressure-insensitive (β = 0.0), that means $C_{\text{emit}} = q_j = Q_{ext}$ (L/s/m$^{0.0}$ = L/s) and $(H_P - z)_j^{0.0}$ = 1.

2.7 Solution by Newton-Raphson method

In equation (20) the only unknown variable H_P cannot be directly calculated because of its non-linearity, so that Newton-Raphson (NR) method should be applied. The NR method is a powerful technique for solving equations numerically. Like so much of the differential calculus, it is based on the simple idea of linear approximation. The NR iteration is the following: let x_0 be a good estimate of H_P and let $H_P = x_0 + h$. Since the true root is H_P, and $h = H_P - x_0$, the number h measures how far the estimate x_0 is from the truth. Since h is "small", we can use the linear (tangent line) approximation to conclude that:

$$0 = f(H_P) = f(x_0 + h) \approx f(x_0) + hf'(x_0) \tag{21}$$

Where:

$$H_P = x_0 + h \approx x_0 - \frac{f(x_0)}{f'(x_0)} \tag{22}$$

The new improved estimate x_1 of H_P is therefore given by:

$$x_1 = x_0 - \frac{f(x_0)}{f'(x_0)} \tag{23}$$

Continue in this way, if x_N is the current estimate, then the next estimate x_{N+1} is given by:

$$x_{N+1} = x_N - \frac{f(x_N)}{f'(x_N)} \tag{24}$$

The application of formula (24) is for solving equations of the form $f(x)$ = 0. The solution is obtained after some calculations until when a pre-specified control value is satisfied.

3. Results

3.1 Example of application 1

The example pipe network consists of a constant level reservoir (upstream) with H_0 = 100 (m), 5 pipes in series and water demands at nodes 2 to 6 [6]. The transient flow is generated by the decrease of the demand at junction 6 in 1 (s). The **Figure 3** and **tables 1** and **2** show the pipe network example and the system data, respectively [6]. The **Figures 4** and **5** show the pressure as function of time at junctions 2, 4 and 6 according to following scenarios:

Scenario 1: pressure-insensitive demand. In this case the pressure-insensitive demand (q_0) in junctions 2 to 6 means taking into account β = 0. For that reason, water demands on nodes 2 to 6 are kept constant and equal to 0.2 (m^3/s) during the simulation time.

Scenario 2: pressure-sensitive demand. In this case equation (20) is solved via NR in order to model the pressure-sensitive demand in junctions 2 to 6, taking into account β = 0.5 such as is recommended by some authors like Jung et al. [6].

In both scenarios the simulation time step is Δt = 0.2 (s), $\Delta x = L/N$ = 1000 / 5 = 200 (m) and the Courant number in pipes 1 to 5 is: $C_n = a \cdot \Delta t/\Delta x$ = 1,000 · 0.2 / 200 = 1.0. Steady-state flow was calculated using EPANET [10]. In the analyzed example, the general sequence of events is the following: after creating the initial surge, the surge wave of the pressure-insensitive demand was propagated without any disturbance except that the friction loss along the pipeline caused a slight attenuation, as is seen in **Figure 4**. On the other hand, the surge wave of the pressure-sensitive demand experienced dramatic pressure attenuation when it passed the junctions (**Figure 5**). According to Jung et al. [6], this is because the positive surge caused a great discharge (higher than the constant demand) through the demand node, and then the demand increase caused a negative surge that was propagated in both upstream and downstream directions. Therefore, the negative surge created from the pressure-sensitive demand interacted with the initial positive surge, causing some pressure dissipation.

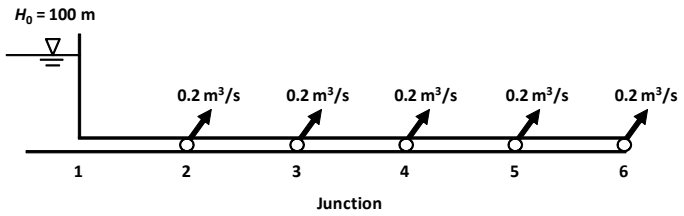

Figure 3 A small pipeline system (adapted from [6]).

Table 1 Pipes data (adapted from [6]).

Pipe number	Diameter D (mm)	Length L (m)	Flow Q_0 (L/s)	Friction factor f	Wave speed a (m/s)
1	1,000	1,000	1,000	0.016	1,000
2	1,000	1,000	800	0.016	1,000
3	1,000	1,000	600	0.016	1,000
4	1,000	1,000	400	0.016	1,000
5	1,000	1,000	200	0.017	1,000

Table 2 Junctions data (adapted from [6]).

Junction number	Initial piezometric head H_0 (m)	Elevation z (m)	Demand q_0 (L/s)
1	100.00	0	0.0
2	98.71	0	200
3	97.88	0	200
4	97.40	0	200
5	97.19	0	200
6	97.13	0	200

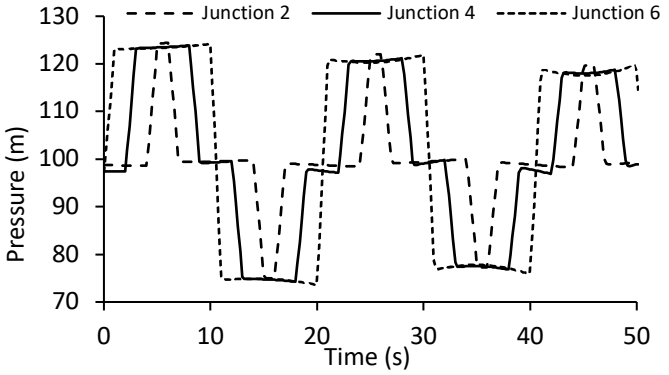

Figure 4 Pressure head profiles using pressure-insensitive demand. (β = 0).

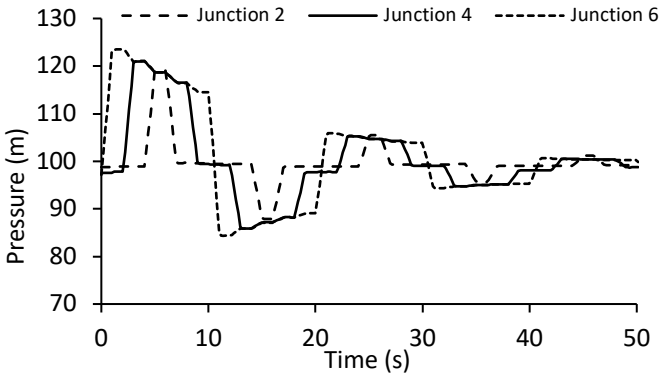

Figure 5 Pressure head profiles using pressure-sensitive demand. (β = 0.5).

When the initial positive surge reached the upstream reservoir, the behavior of pressure-sensitive demand was the opposite of the initial positive surge because the positive surge was converted into a negative surge. The negative surge caused a lower discharge (lower than the constant demand) through the demand node, and then the resulting decrease demand caused a positive surge, which dissipated the reflected negative surge from the reservoir. **Table 3** shows the maximum positive surge (obtained by subtracting the maximum transient pressure from the initial steady pressure), the maximum negative surge (obtained by subtracting the minimum transient pressure from the initial steady pressure), and their differences for junctions 2, 4 and 6 and for both pressure-insensitive and pressure-sensitive demand analyses. The results in **Table 3** show a good fit level with the results reported by Jung et al. [6].

Table 3 Maximum positive and negative surges (PID = pressure-insensitive demand, PSD = pressure-sensitive demand).

Junction number	Maximum positive surge		Minimum positive surge	
	PID	PSD	PID	PSD
2	25.7	20.3	–23.8	–10.8
4	26.5	23.6	–23.2	–11,5
6	27.1	26.4	–23.5	–12.8

3.2 Example of application 2

Example 1 served to verify the correct functioning of the proposed algorithm. Next, the algorithm will be tested in the complex pipe network shown in **Figure 6,** which consists of 45 pipes, 29 junctions, 1 constant level reservoir and a valve that closes in 1 (s). In junctions 8 and 21 there are constant water demands of 50 (L/s) and 15 (L/s), respectively. In the junctions 4, 11, 17, 23, 24 and 28 there are water demands of magnitude q_0 = 5 (L/s) each one. All the nodes have elevation 0 (m). The **tables 4** and **5** show the junctions and pipes data, respectively. The pipe network discretization considers Δt = 0.05760875 (s) and a N value that ranges between 2 and 14 depending on the lengths of the pipes. Steady-state flow was calculated using EPANET [10]. The system was solved by the MOC with C_n = 1.0 in all pipes. Figures 7 and 8 show the pressure as function of time at junctions 11, 17, 24 and 28 according to the following scenarios:

Scenario 1: pressure-insensitive demand. The transient flow is generated by valve closure in 1.0 (s). In this case the pressure-insensitive demand (q_0) in junctions 4, 11, 17, 23, 24 and 28 means taking into account β = 0.0. In nodes 8 and 21 the water demand also keeps pressure-insensitive during the simulation time.

Scenario 2: pressure-sensitive demand. The transient flow is generated by valve closure in 1.0 (s). In this case equation (20) is solved via NR in order to model the pressure-sensitive demand in junctions 4, 11, 17, 23, 24 and 28, taking into account β = 0.5. In nodes 8 and 21 the water demand keeps pressure-insensitive during the simulation time.

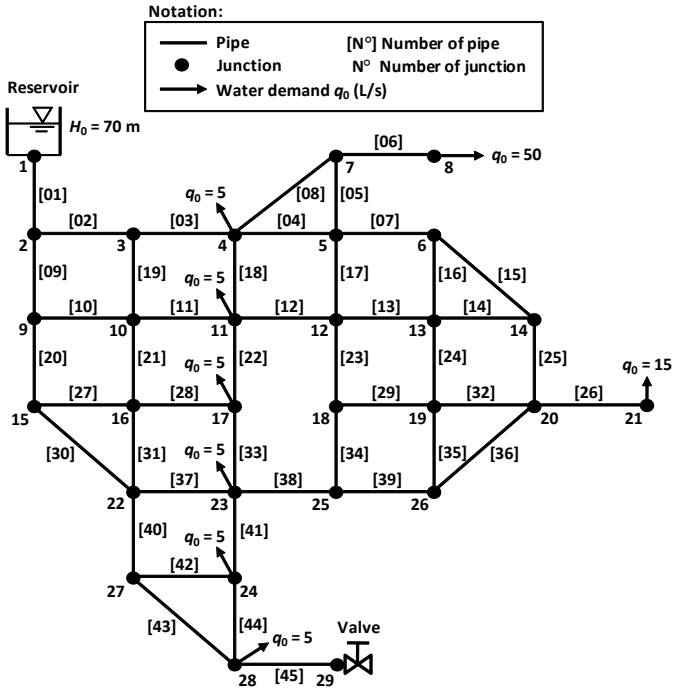

Figure 6 Pipe network example.

Table 4 Junctions data.

Junction number	Initial piezometric head H_0 (m)	Demand q_0 (L/s)
1	70.00	0
2	58.70	0
3	50.44	0
4	44.25	5
5	40.88	0
6	39.11	0
7	40.18	0
8	38.76	50
9	54.55	0
10	49.59	0
11	46.57	5
12	42.69	0

Table 4 (cont.) Junctions data.

Junction number	Initial piezometric head H_0 (m)	Demand q_0 (L/s)
13	38.90	0
14	37.87	0
15	50.12	0
16	45.42	0
17	41.28	5
18	38.03	0
19	36.97	0
20	34.30	0
21	31.39	15
22	40.69	0
23	36.00	5
24	35.63	5
25	36.59	0
26	36.36	0
27	37.56	0
28	34.13	5
29	32.72	0

Table 5 Pipes data.

Pipe number	Diameter D (mm)	Length L (m)	Flow Q_0 (L/s)	Friction factor f	Wave speed a (m/s)
1	200	120	145.00	0.017	1,036.893
2	150	120	58.05	0.019	1,038.224
3	150	120	50.13	0.019	1,038.672
4	110	120	16.16	0.021	187.665
5	150	120	16.21	0.020	188.448
6	200	120	50.00	0.018	187.774
7	75	120	4.19	0.025	1,040.560
8	150	169.71	33.79	0.019	980.057
9	200	120	86.95	0.018	186.597
10	150	120	44.75	0.019	1,038.976
11	150	120	34.63	0.020	1,039.549
12	110	120	17.39	0.021	187.535
13	75	120	6.23	0.024	206.892
14	75	120	3.15	0.025	207.589
15	75	169.71	2.88	0.026	209.770

Table 5 (cont.) Pipes data.

Pipe number	Diameter D (mm)	Length L (m)	Flow Q_0 (L/s)	Friction factor f	Wave speed a (m/s)
16	75	120	1.31	0.037	208.005
17	75	120	4.23	0.024	207.344
18	75	120	4.83	0.024	207.208
19	110	120	7.92	0.024	188.532
20	150	120	42.2	0.019	1,039.121
21	110	120	18.04	0.021	692.441
22	75	120	7.41	0.024	206.624
23	75	120	6.94	0.024	206.731
24	75	120	4.38	0.025	207.310
25	75	120	6.03	0.024	206.937
26	110	120	15.00	0.021	187.787
27	110	120	19.21	0.021	692.318
28	110	120	17.98	0.021	692.447
29	75	120	3.19	0.025	207.580
30	110	169.71	22.99	0.021	979.550
31	110	120	19.27	0.021	187.337
32	75	120	5.19	0.024	207.127
33	110	120	20.39	0.021	187.220
34	75	120	3.75	0.027	207.453
35	75	120	2.38	0.029	207.763
36	75	169.71	3.78	0.024	209.566
37	75	120	6.96	0.024	206.726
38	75	120	2.35	0.029	207.770
39	75	120	1.40	0.025	207.985
40	150	120	35.30	0.020	1,039.511
41	200	120	24.70	0.020	1,040.722
42	75	120	4.38	0.025	207.310
43	150	169.71	30.92	0.020	980.219
44	150	120	24.08	0.020	1,040.146
45	200	120	50.00	0.018	1,039.917

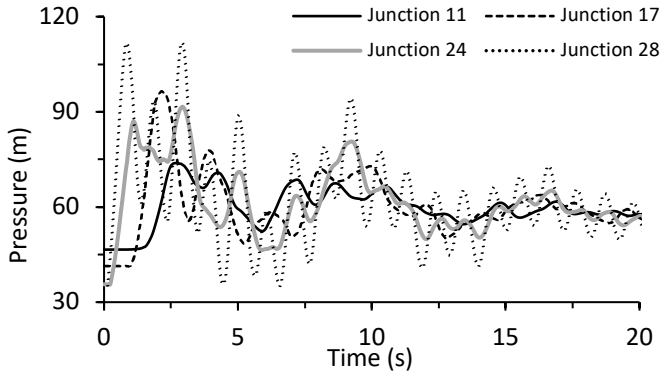

Figure 7 Pressure head profiles (β = 0.0)

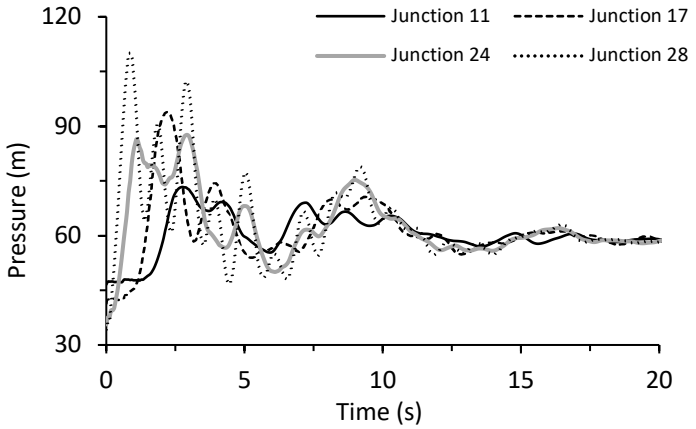

Figure 8 Pressure head profiles (β = 0.5)

When comparing Figures 7 and 8 it is verified that PSD reduce the extreme pressures magnitude, which tend to decay quickly after 5 (s) of simulation time. Table 6 shows a comparison between maximum positive and negative surges when PID and PSD scenarios are simulated.

Table 6 Maximum positive and negative surges (PID = pressure-insensitive demand, PSD = pressure-sensitive demand).

Junction number	Maximum positive surge		Minimum positive surge	
	PID	PSD	PID	PSD
11	27.3	26.8	0.0	−0.5
17	55.2	52.7	0.0	−0.3
24	55.9	51.9	0.0	0.0
28	77.5	75.8	0.0	0.0

4. Conclusions

Each hydraulic modeling exercise requires certain assumptions and approximations to simplify the problem and facilitate obtaining the solution. The assumption of pressure-insensitive demand has been widely applied to surge analysis but this modeling approach may be problematic because it ignores the implicit relationships between demand and pressure inherent in actual pipe systems [6]. The pressure transients can drastically alter the local pressures, which in turn can significantly affect the magnitude of nodal demands that can be extracted. The assumption of pressure-insensitive demand exaggerates a surge wave in the system, leading to conservative solutions which could lead to overdesign surge-protection devices. An over designed system sometimes can be more detrimental than an under designed one because the over designed hydraulic devices themselves may deteriorate the surge response of the system. A more realistic water hammer simulation should always consider pressure-sensitive demand behavior in some singular network nodes, even when this approach may increase the numerical problem complexity. For that reason, in some cases could be more efficient to apply the pressure-sensitive demand approach only on network nodes which often present very high and fast flow variations, like sudden demand due to fire cases. Another application for pressure-sensitive demand approach is for more accurately estimate contaminant intrusion in WDS [6]. Contaminants can intrude into pipes through leaks during a negative pressure transient; the surge model using pressure-sensitive demand can simulate the location, amount and duration of these intrusions. The application of pressure-sensitive demand approach in very large and complex pipe networks may affect the execution time because the Newton-Raphson method must be applied in order to calculate the pressure-sensitive demand in hundreds or thousands of significant junctions, this in each time step. In the example 1 the execution time for scenarios 1 and 2 was 0.7 (s) and 0.8 (s), respectively. In example 2, the execution time was 19.7 (s) and 20.2 (s) for scenarios 1 and 2, respectively. Water hammer program was carried out in a standard PC of 32 bits with a processing speed equal to 1.66 (GHz). Proposed algorithm needs the following improvements, such as the inclusion in the model of the cross-correlation (interdependence) between forthcoming demands, and to implement an algorithm that allows calculate the transient flow in systems with uniformly distributed demands, not only in the junctions of the pipe network but also on pipe internal nodes without having to alter the discretization initially adopted for the system. This is because it is well known that water demands are distributed along the pipelines, and that their allocation at the junctions just corresponds to a simplification generally accepted for modeling purposes. This would allow having simulations closer to reality. Finally, the NR method sometimes it may not converge due to different reasons. Sometimes it may overlook the root you are trying to find and converge to a different root, and sometimes it may fail to converge altogether. In this sense, NR method is very sensitive to β value in equation (20), being recommendable always to work with β equal to or near 0.5.

5. References

[1] Araujo L.S., Ramos H., Coelho S.T. (2006). Pressure control for leakage minimisation in water distribution systems management. Water Resources Management, 20: 133-149.

[2] Brown K. (2007). Modelling leakage in water distribution systems. Master of Science Thesis. The Florida State University.

[3] Chaudhry M.H. (1979). Applied hydraulic transients, p. 266. New York: Van Nostrand Reinhold. * p. 27-33.

[4] Chaudhry M.H., Hussaini M.Y. (1985). Second-order accurate explicit finite-difference schemes for waterhammer analysis. Journal of Fluids Engineering, 523-529.

[5] Jowitt P.W., Xu C. (1990). Optimal valve control in water-distribution networks. Journal of Water Resources Planning and Management, 116(4).

[6] Jung B.S., Boulos P.F., Wood D.J. (2009). Effect of pressure-sensitive demand on surge analysis. Journal of AWWA, 101(4): 100-111. http://www.mwhsoft.com/products/surge/papers/jawwaapr09surgepaper.pdf

[7] Karney B.W. (1984). Analysis of fluids transients in large distribution networks. PhD. Thesis. Vancouver: University of British Columbia. http://hdl.handle.net/2429/25312

[8] Karney B.W., McInnis D. (1992). Efficient calculation of transient flow in simple pipe networks. Journal of Hydraulic Engineering, 118(7): 1014−1030.

[9] Larock B.E., Jeppson R.W., Watters G.Z. (2000). Hydraulics of pipeline systems, p. 533. Boca Raton: CRC Press. p* 341.

[10] Rossman L.A. (1993). User's manual for EPANET. Drinking Water Resources Division. Cincinnati: USEPA.

[11] Salgado R., Twyman C., Twyman J. (1992, 8-12 Septiembre). Desarrollo de un algoritmo híbrido para el análisis del escurrimiento impermanente rápido en redes de tuberías a presión. XV Congreso Latinoamericano de Hidráulica (pp. 483-493). Cartagena: IAHR.

[12] Salgado R., Rojo J., Zepeda S. (1993). Extended gradient method for fully non-linear head and flow analysis in pipe networks. Integrated Computer Applications in Water Supply (Vol. 1). New York: John Wiley & Sons. 49-60.

[13] Seyoum A.G., Tanyimboh T.T. (2014). Practical application of pressure-dependent EPANET extension. CUNY Academic Works, pp. 7.

[14] Siew C., Tanyimboh T.T. (2012). Pressure-dependent EPANET extension. Water Resources Management, 26: 1477-1498.

[15] Suribabu C.R., Neelakantan T.R. (2011). Balancing reservoir based approach for solution to pressure deficient water distribution networks. International Journal of Civil and Structural Engineering, 2(2): 639-647.

[16] Twyman J. (2016). Wave speed calculation for water hammer analysis. Obras y Proyectos, UCSC. 20: 86-92. http://dx.doi.org/10.4067/S0718-28132016000200007

[17] Twyman J. (2016, 26-30 Septiembre). Golpe de Ariete en una Red de Distribución de Agua. XXVII Congreso Latinoamericano de Hidráulica (pp. 10). Lima: IAHR (Spain Water and IWHR China).

[18] Twyman J. (2016). Water hammer analysis using the Method of Characteristics. Revista de la Facultad de Ingeniería (Universidad de Atacama), 32(2016): 1-9. http://www.revistaingenieria.uda.cl/publica.php?tipot=1&tipov=2

[19] Twyman J. (2017). Water hammer analysis in a water distribution system. Ingeniería del Agua, 21(2): 87-102. https://doi.org/10.4995/Ia.2017.6389

[20] Twyman J. (2017). Water hammer analysis using a hybrid scheme. Journal of Construction and Civil Engineering RIOC, 7(2017): 16-25. http://www.rioc.cl/index.php/RIOC/article/view/16

[21] Twyman J. (2018). Water hammer analysis using an implicit finite-difference method. Ingeniare, 26(2): 307-318.

[22] Wan W., Mao X. (2016). Shock Wave Speed and Transient Response of PE Pipe with Steel-Mesh Reinforcement. Shock and Vibration, Volume 2016 (2016). Article ID 8705031. http://dx.doi.org/10.1155/2016/8705031

[23] Wylie E.B., Streeter V.L. (1978). Fluid transients, p. 206. New York: McGraw-Hill. Int. Book Co. * p. 22-23.

[24] Wylie E.B. (1984). Fundamental equations of waterhammer. Journal of Hydraulic Engineering, 110 (4): 539-542.

[25] Wylie E. B. (1986). Liquid transient flow in piping systems. In Arndt R.E., Stefan H.G., Farell C., Peterson S.M. (1986). Advancements in Aerodynamics. Fluid Mechanics and Hydraulics, 50-57.